

Production of $\tau\tau jj$ final states at the LHC and the TauSpinner algorithm: the spin-2 case

M. Bahmani¹, J. Kalinowski², W. Kotlarski^{2,3} , E. Richter-Was⁴, Z. Was^{1,a}

¹ Institute of Nuclear Physics, Polish Academy of Sciences, ul., Radzikowskiego 152, Kraków, Poland

² Faculty of Physics, University of Warsaw, Pasteura 5, 02-093 Warsaw, Poland

³ IKTP, Technische Universität Dresden, Zellescher Weg 19, 01069 Dresden, Germany

⁴ Institute of Physics, Jagellonian University, Lojasiewicza 11, 30-348 Cracow, Poland

Received: 22 August 2017 / Accepted: 19 December 2017
© The Author(s) 2018. This article is an open access publication

Abstract The TauSpinner algorithm is a tool that allows one to modify the physics model of the Monte Carlo generated samples due to the changed assumptions of event production dynamics, but without the need of re-generating events. With the help of weights τ -lepton production or decay processes can be modified accordingly to a new physics model. In a recent paper a new version TauSpinner ver. 2.0.0 has been presented which includes a provision for introducing non-standard states and couplings and study their effects in the vector-boson-fusion processes by exploiting the spin correlations of τ -lepton pair decay products in processes where final states include also two hard jets. In the present paper we document how this can be achieved taking as an example the non-standard spin-2 state that couples to Standard Model particles and tree-level matrix elements with complete helicity information included for the parton-parton scattering amplitudes into a τ -lepton pair and two outgoing partons. This implementation is prepared as the external (user-provided) routine for the TauSpinner algorithm. It exploits amplitudes generated by MadGraph5 and adapted to the TauSpinner algorithm format. Consistency tests of the implemented matrix elements, re-weighting algorithm and numerical results for observables sensitive to τ polarisation are presented.

1 Introduction

With increasing statistics collected by the LHC experiments the interests to explore final states with τ -leptons gain importance. Because of the high mass and their decays, τ -leptons may provide a sensitive window to physics beyond the Standard Model predictions. The TauSpinner algorithm,

started with Ref. [1], provides a powerful tool to investigate characteristics of final states with τ -leptons due to modifications in underlying physics models. This is obtained with the help of weights attributed to each event from collision data or Monte Carlo generated, and thus without repeating the detector response simulation with each variant of the physics model. An approach where physics assumption variation can be introduced with weights is useful for many modern data analysis techniques. The first version of TauSpinner re-weighting found its application in the domain of Standard Model measurements [2] but also for New Physics limits established for simple $2 \rightarrow 2$ parton level processes [3]. Later, in [4,5], TauSpinner was found useful for discussion of CP sensitive massively multi-dimensional observables in the frame of machine learning techniques [6]. In a recent paper [7] an extended version of TauSpinner 2.0.0 was presented which now includes hard processes featuring tree-level parton matrix elements for production of a τ -lepton pair and two jets. It was prepared as a tool to be helpful for studying spin effects in processes of Standard Model and searches of New Physics, like in Refs. [9,10]. It found also tempting applications in the domain of implementation and discussion of variants for Standard Model electroweak calculation schemes used in simulation programs ([7], see also [8]), and in experimental applications for Standard Model measurements [11–14].

Before discussing TauSpinner as a tool for studying observables of New Physics let us briefly recall some virtues of the TauSpinner algorithm. Since τ -leptons cannot be observed directly due to their short life-time with more than 20 different decay channels, each with somewhat distinct signature, recalculating and reanalyzing observables involving τ decays is time consuming. However, the τ -lepton spin polarisation can be inferred from their decays, contrary to the case of electron or muon signatures. Spin effects can pro-

^ae-mail: Z.Was@cern.ch

vide a better insight into the nature of the underlying physics. Therefore efforts to explore these phenomena are worth pursuing. `TauSpinner` allows one to greatly simplify the task of exploring the experiments' sensitivity. Evaluation of measurements significance due to different New Physics models can be performed with the help of event weights. Technical aspects of the algorithm in the case of configurations with two jets accompanying a τ -lepton pair have been covered in [7].

The purpose of the present paper is to document how the user can apply the `TauSpinner` algorithm to the physics model considered. To this end, we take as a case study a non-standard spin-2 object coupled to SM particles. We analyze its production in proton–proton collisions and decay to a τ -lepton pair, addressing also the question to what extent τ polarisation can be exploited to investigate its nature. We demonstrate how `TauSpinner` can facilitate such studies with the help of matrix elements for that model (or any other, provided by the user). Corresponding weight can be calculated and applied to each event of samples with full experiment simulation chains. As it is practically impossible to repeat simulations with detector response effects included for each new physics hypothesis, our procedure is beneficial and may be the only available option for the general use despite its limitations. `TauSpinner` algorithm can also be applied on measured data events, e.g. in the context of embedded τ lepton techniques [15].

The paper is organised as follows: Sect. 2 and Appendix A provide details of `TauSpinner` which were not discussed in Ref. [7], or treated very briefly, but they are of importance for the case of New Physics models. Section 3 documents details of the tree-level matrix elements used for the calculation of spin-2 object exchange amplitudes which are later passed for weights calculation in $pp \rightarrow \tau\tau jj$ events. The implemented functionality is based on automatically produced FORTRAN code from the `MadGraph5` package [16] similarly to processes of the Drell–Yan type and to the Standard Model Higgs boson production in vector-boson-fusion processes (VBF). We explain details of the modification which we have introduced to the code of amplitudes generated with `MadGraph5` (version `MG5_aMC_v2.4.3`). Section 4 and Appendix B are devoted to numerical results. First, tests for fixed kinematic configurations are recalled. Later, definitions of observables are given, and some distributions are presented. In Sect. 5 numerical results sensitive to τ polarisation are presented taking the single-prong decay $\tau^\pm \rightarrow \pi^\pm \nu$ channel as a spin analyser. Section 6 summarises and concludes the paper.

2 The `TauSpinner` weight $w_{\text{prod}}^{A \rightarrow B}$

`TauSpinner` does not provide methods to generate pp collision events. Therefore, the necessary input for `TauSpinner`

consists of a series of events, which could be of a process different from the required one but with the same outgoing final states. The events must contain information on the four-momenta of (two) outgoing jets and τ -leptons with their decay products, which is necessary for the calculation of the hard process matrix elements. Flavours of incoming/outgoing partons are determined by the algorithm – there is no need to read them from the generated events. The sum over all possible configurations, weighted with PDFs, is performed. On the other hand, the information on the decay products of τ -leptons is needed for the evaluation of spin effects. Using this input, the value of the corresponding matrix elements can be calculated on the event by event basis and in particular the corresponding spin weight. As discussed in detail in Ref. [7], for each event

$$j_i(p_1)j_j(p_2) \rightarrow j_k(p_3)j_l(p_4)\tau^+\tau^-, \quad (1)$$

where j stands for a quark, antiquark or a gluon, the algorithm calculates the weight

$$w_{\text{prod}}^{A \rightarrow B} = \frac{\sum_{ijkl} \frac{1}{\Phi_{\text{flux}}^{i,j}} f_i^B(x_1) f_j^B(x_2) |M_{ijkl}^B(\{p\})|^2 d\Omega(\{p\})}{\sum_{ijkl} \frac{1}{\Phi_{\text{flux}}^{i,j}} f_i^A(x_1) f_j^A(x_2) |M_{ijkl}^A(\{p\})|^2 d\Omega(\{p\})}, \quad (2)$$

which represents, for a given phase-space point ($\{p\}$) = ($p_1, p_2, p_3, p_4, p_{\tau^+}, p_{\tau^-}$), the ratio due to the matrix element used in the generation of the sample for process (A) and the matrix elements corresponding to a New Physics model¹ (B). The evaluation of the weight in Eq. (2) requires the knowledge of contributions from all possible parton level configurations ($ijkl$) weighted with parton density functions $f_{i/j}^{A/B}(x)$ and flux factors $\Phi_{\text{flux}}^{i,j}$. The sums run over both gluons and quark flavours alike. Note, however, that the flavour is passed to the user-provided matrix-element routine and flavour dependence can be introduced there. For the details and explanation of the notation used in Eq. (2) we refer to [7]. For the purpose of calculating $w_{\text{prod}}^{A \rightarrow B}$ we sum over all possible helicity configurations of outgoing τ -leptons. An event generated for the process (A), when weighted with $w_{\text{prod}}^{A \rightarrow B}$ becomes an event of the process (B). Spin effects in τ decays have to be introduced separately, with `TauSpinner` main spin weight WT , as explained in Appendix A.

The following details need to be stressed when selecting a suitable process (A) given the target process (B). For a narrow resonance, like the Higgs state, the values of the matrix elements vary greatly with the invariants built from the final-state four-momenta. Therefore the numerical stabilisation needs to be kept in mind. The `TauSpinner` algorithm

¹ It can also be a variant of the Standard Model initialisation, e.g. in terms of distinct electroweak schemes.

must reconstruct the invariant mass of the resonance with a precision better than 1–2 MeV from the four-momenta of final-state particles, whose energies may lie in the range of TeV. Double precision may be needed since otherwise some invariants may be inappropriately evaluated due to simple computer rounding errors. A user has to ensure that the re-weighting indeed works in the interesting regions of the phase space. In particular, that the phase space is populated for both processes (A) and (B) with not too massively distinct distributions, and that the distribution enhancements due to intermediate resonances or collinear or soft singularities have similar (matching) structure. The checks listed above require hard process information only.

3 New Physics model of (2 → 4) process

As a case study we consider a simplified model of a massive gauge singlet spin-2 object X coupled to the SM gauge bosons. We use this model to demonstrate how to prepare and test external matrix element to be used by TauSpinner algorithm.

Scenarios with spin-2 objects have been already intensively studied in the literature in the context of LHC phenomenology [18–20], though none of the studies was dedicated to the analysis of X decays into τ final states. Note, however, that, for a general study of a “Higgs”-like resonance and its parity in vector-boson-fusion processes with a τ pair as a decay product, experimental results are becoming available [21, 22].

In Ref. [3] we studied a Drell–Yan-like production of τ 's through a hypothetical spin-2 object X . Building on our previous work, we study now the X production in the VBF topology, followed by $X \rightarrow \tau^+\tau^-$ decay. We start by extending the Lagrangian of Ref. [3] by a set of gauge invariant dimension 5 operators, coupling the field X to gauge boson field strength tensors B , W and G as

$$\mathcal{L} \ni \frac{1}{F} X_{\mu\nu} (g_{XBB} B^{\mu\rho} B_{\rho}^{\nu} + g_{XWW} W^{\mu\rho} W_{\rho}^{\nu} + g_{Xgg} G^{\mu\rho} G_{\rho}^{\nu}), \tag{3}$$

where the group indices are implicitly summed over (where appropriate). The parameter F , set to 1 TeV, is introduced to keep the coupling constants dimensionless. Note that we are agnostic on the origin of the state X , in particular we do not claim it is connected to gravity. Hence we do not couple it to the entire energy momentum tensor and couplings g_X are kept as free parameters. This is in contrast to, for example Ref. [23], where the X field is coupled to the energy momentum tensor of quantised SM.

After the electroweak symmetry breaking, operators in Eq. (3) generate vertices with couplings of X to photons,

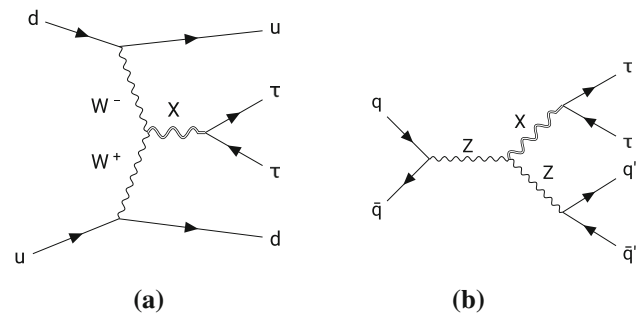


Fig. 1 Topologies of Feynman diagrams for X production through its coupling to gauge bosons. Similar diagrams, with different combinations of W^{\pm} 's, Z 's, photons and quark flavours, also exist

W^{\pm} 's, Z 's and gluons; the explicit formulas for those couplings can be found in [20]. Since in this work we focus on technical aspects of incorporating the couplings of X to the EW gauge bosons, for numerical tests of the correctness of the matrix element implementation, we set $g_{XBB} = g_{Xgg} = 0$. Relevant diagram topologies are shown in Fig. 1: for the VBF process (Fig. 1a) and the X -strahlung process (Fig. 1b).

3.1 Generating matrix-element code using MadGraph5

The extension of the SM by spin-2 field coupled to the gauge fields as in Eq. (3), including also coupling of the X field to quarks and τ -leptons from [3], is encoded into a FeynRules [24] model. The FeynRules model file, together with its UFO output [25], is available in supplementary materials of the arXiv version of this reference. The UFO model is used to generate squared matrix elements using MadGraph5, employing the spin-2 support of the HELAS library [26]. This is done with the following set of commands:

```
(a) import model spin2_w_CKM_UFO
(b) let "multiparticles" containers already include all massless partons

p = g u c d s u~ c~ d~ s~
j = g u c d s u~ c~ d~ s~

(this is so by default)
(c) generate spin 2 matrix elements

generate p p > j j x QED<=99
QCD<=99 NPgg<=99 NPqq<=99
NPVV<=99, x > ta+ ta-

(d) write the output to disk in MadGraph's standalone mode using

output standalone "directory name"
```

NPgg, NPq \bar{q} and NPVV parameters control the maximum number of g_{Xgg} , $g_{Xq\bar{q}}$ and g_{XWW} , g_{XBB} couplings, respectively. Limiting them by 99 effectively means that their number is not restricted. The model includes the CKM matrix in the Wolfenstein parametrisation. As was stated above, for numerical tests we restrict ourselves setting $g_{XBB} = g_{Xgg} = 0$, though we stress again that the matrix element, coded as an example user process, contains all of them; see Appendix B for actual initialisation of coupling constants.

3.2 Integrating matrix-element code into **TauSpinner** example

The matrix-element code is based on automatically produced FORTRAN subroutines by MadGraph5 package, similarly as it has been done for processes of the Drell–Yan type and of the Standard Model Higgs boson production in vector-boson-fusion (VBF)/Higgs-strahlung processes [7]. In the spin-2 case they have also been manually modified and adapted to avoid name clashes. This technical complication is a consequence of the fact that the C++ user function for the spin-2 matrix element calls FORTRAN code created by MadGraph5. We therefore cannot profit from the namespace functionality of C++ as a natural solution to this problem. Some name changes are necessary, as explained below. The corresponding code is stored in the directory `TauSpinner/examples/example-VBF/SPIN2/ME`.

The generated codes for the individual sub-processes are grouped together into subroutines, depending on the flavour of initial-state partons, and named accordingly. For example,

```
SUBROUTINE DCX_S2 ( P, I3, I4, H1, H2, ANS )
```

encompasses the X production processes initiated by the $d\bar{c}$ partons. We follow our previous convention [7] where the symbol X in the subroutine or internal function name after the letter U, D, S or C means that the corresponding parton is an antiquark, i.e. $UXCX$ corresponds to processes initiated by $\bar{u}\bar{c}$ partons, while GUX corresponds to processes initiated² by $g\bar{u}$. The $S2$ stands explicitly for the production of spin-2 X state. The input variables are a real matrix $P(0:3, 6)$ for four-momenta of incoming and outgoing particles, integers $I3, I4$ for the Particle Data Group (PDG) identifiers for final-state parton flavours and integers $H1, H2$ for the outgoing τ helicity states. Before integrating these subroutines into the `TauSpinner` program, a number of modifications have been done for the following reasons:

- (a) Since MadGraph5 by default sums and averages over spins of incoming and outgoing particles, while we are interested in τ spin states, the generated codes have

to be modified to keep track of the τ polarisation, i.e. indices/helicities $H1$ and $H2$.

- (b) Moreover, since the subroutines and internal functions generated by MadGraph5 have the same names for all sub-processes, namely `SMATRIX(P, ANS)`, the names had to be changed to be unique. As an example, the subroutine name for the sub-process $u\bar{d} \rightarrow c\bar{d}X, X \rightarrow \tau^+\tau^-$ was changed to `UDX_CD_X_S2(P, H1, H2, ANS)`. These subroutines will be called by the subroutine

```
UDX_S2(P, 4, -1, H1, H2, ANS).
```

- (c) For a pair of final-state parton flavours $k \neq l$, the MadGraph5 generated codes have been obtained for a definite ordering (k, l) , but not for (l, k) , to reduce the number of generated configurations. When `TauSpinner` is invoked, the configuration of outgoing partons is unknown and it takes into account both possibilities: thus a compensating factor $\frac{1+\delta_{l,k}}{2}$ has to be introduced due to the way of organizing the sum in Eq. (2) and in Ref. [7].
- (d) For the calculation of matrix elements MadGraph5 is using ALOHA functions [27] stored in FORTRAN subroutines. Since some of these functions have originally names identical to functions in the `TauSpinner` source code for the implementation of the Standard Model VBF/Higgs-strahlung production, names of those functions have to be modified also to avoid any name conflicts. Therefore ALOHA functions stored in `TauSpinner/examples/example-VBF/SPIN2/ME/Spin2_functions.f` are changed by adding the “_S” suffix to the original names of subroutines, for example `FFV4_0` is changed to `FFV4_0_S`.

Table 1 summarises the naming convention for the files. At the parton level each of the incoming or outgoing partons can be one of the flavours: $\bar{c} \bar{s} \bar{u} \bar{d} g d u s c$, with Particle Data Group (PDG) identifiers: $-4, -3, -2, -1, 21, 1, 2, 3, 4$, respectively. For processes with two incoming partons, two outgoing τ -leptons and two outgoing partons, there are 9^4 possibilities, most of them evaluating to 0 or obtainable one from another, by relations following from CP symmetries and/or permutations of incoming and/or outgoing partons.

For each point in the parton level phase space, consisting of all incoming and outgoing four-momenta as well as their flavours, depending on the user choice, one of two variants of processes (i.e. pairs of matrix elements) may be used by `TauSpinner` executable. That is, the Drell–Yan variant (standard, and user-provided New Physics matrix elements) or Higgs-like variant (again standard, and user-provided one).³

² X in this context should not be confused with the spin-2 field X .

³ The prototype is implemented in the example; see Appendix A.1.

Table 1 List of implemented processes contributing to the spin-2 X particle production, grouped into categories which differ by flavours of incoming partons. For each category, the names of FORTRAN files calculating squared matrix elements, for given flavour configuration of incoming partons, are given in the second column. Examples of processes in each category are given in the last column

Category of matrix elements	Corresponding FORTRAN files	Processes
(1)	<i>GG_S2.f</i>	$gg \rightarrow \sum_f q_f \bar{q}_f X$
(2)	<i>GC_S2.f, GU_S2.f</i>	$gq_f \rightarrow gq_f X$
(3)	<i>GcX_S2.f, GUX_S2.f</i>	$g\bar{q}_f \rightarrow g\bar{q}_f X$
(4)	<i>DD_S2.f, UD_S2.f, UU_S2.f,</i> <i>CC_S2.f, CS_S2.f,</i> <i>SS_S2.f CD_S2.f,</i> <i>CU_S2.f, SD_S2.f, SU_S2.f</i>	$q_{f_1} q_{f_2} (\bar{q}_{f_1} \bar{q}_{f_2}) \rightarrow q_{f_1} q_{f_2} (\bar{q}_{f_1} \bar{q}_{f_2}) X$
(5)	<i>DDX_S2.f, UDX_S2.f, UUX_S2.f</i> <i>CCX_S2.f, CSX_S2.f, DCX_S2.f,</i> <i>SCX_S2.f, SSX_S2.f, UCX_S2.f,</i> <i>CDX_S2.f, CUX_S2.f, SDX_S2.f,</i> <i>SUX_S2.f</i>	$q_{f_1} \bar{q}_{f_2} (\bar{q}_{f_1} \bar{q}_{f_2}) \rightarrow q_{f_1} \bar{q}_{f_2} (\bar{q}_{f_1} \bar{q}_{f_2}) X$ $q_{f_1} \bar{q}_{f_2} (\bar{q}_{f_1} \bar{q}_{f_2}) \rightarrow gg X$

Certain limitations need to be kept in mind. In practice, it is simply impossible to obtain a statistically significant distribution of weighted events for the particular model under study in the region of phase space where the original sample is sparse or possibly no events are present at all. In particular, the mass and width of the Higgs-like resonance need to coincide with (or be close to) those of the Higgs. Also, the algorithm is expected to be used in regions of the phase space where the kinematic distributions of the original and New Physics models are not massively different.

4 Tests of implementation of external matrix elements

Once the user-provided external matrix elements are prepared, numerical tests are necessary if it indeed has been implemented properly into the TauSpinner environment. In the following we discuss such tests, using spin-2 matrix elements of Xjj production as an example. We start from the technical one and continue with more physics oriented ones. Finally we will demonstrate the limitations of the method.

4.1 Test of matrix elements using fixed kinematic configuration

For checking the consistency of the implemented codes generated with MadGraph5 and modified as explained in Sect. 3.2, we have chosen a single event with fixed kinematic configuration at the parton level. We have calculated the matrix elements squared for that event and for all possible helicity and parton flavour configurations, using the code implemented as user example. We compared results with the

numerical values obtained directly from MadGraph5. The agreement of at least 6 significant digits has been confirmed.

4.2 Tests of matrix elements using series of generated events

As further tests of the internal consistency of external matrix-element implementation, we have explored the re-weighting procedure by comparing a number of kinematic distributions obtained directly or re-weighted with $w_{\text{prod}}^{A \rightarrow B}$ from series of 10M events generated by MadGraph5 for X particle and Higgs boson. Samples were generated for pp collisions at 13 TeV using CTEQ6L1 PDFs. The mass of both X particle and Higgs boson was set to 125 GeV and the width to 5.75 MeV. The details of cuts and MadGraph5 initialisation used for the sample generation are given in Ref. [17]. On the generated events the following further selections were applied: $m_{jj\tau\tau} < 1500 \text{ GeV}$, $p_T^{\tau\tau} < 600 \text{ GeV}$ and $m_{jj} < 800 \text{ GeV}$ (loose selection) to eliminate excessive weight regions of the phase space, or eliminating also $Z \rightarrow jj$ or $W \rightarrow jj$ resonance peaks $100 < m_{jj} < 800 \text{ GeV}$ (tight selection).

Before commenting on the actual results let us point to the size of statistical errors⁴ which reflect comparability of the H (process A) and X (process B) samples. Errors are always larger than what could be expected from weight-one samples of similar size. This effect can be understood better with the weight distributions shown in Fig. 2. In both cases of re-weighting: from H to X (top panel) and X to H (bottom panel), one can observe a constant slope on this double logarithmic plot with clear sharp upper end. With such a

⁴ The statistical errors of all histograms, including the ones using weighted events, were evaluated by the standard algorithms of the root library [28].

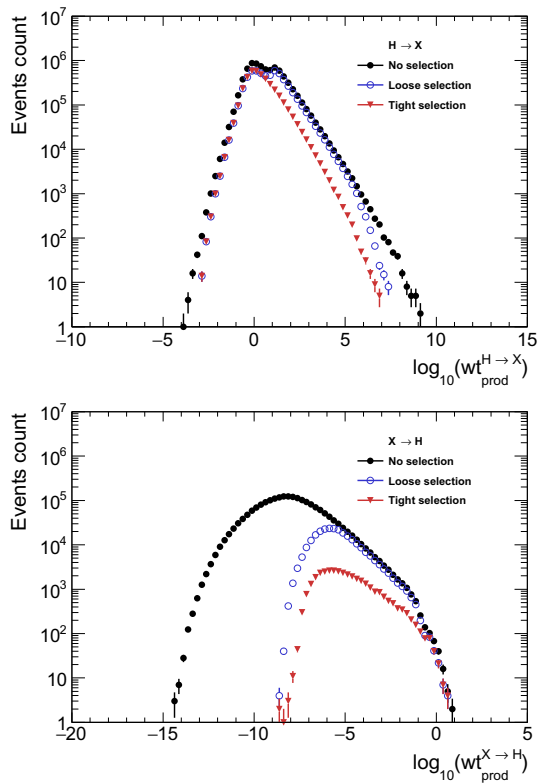


Fig. 2 Weight distribution for H sample re-weighted to X (top panel) and for the X sample re-weighted to H (bottom panel). If the distribution featured a long tail extending to high weights, it would indicate a problem with re-weighting in regions of the phase space where the ratio of the matrix element (B) with respect to the one of the original sample (A) is too large in comparison with the typical event

spectrum of weights a statistically sensible calculation of the cross sections and distributions may still be possible. If a tail of events with ever higher weights would continue to form when increasing the size of the samples, statistical errors would never decrease. This happens, for example, if in some sub-dimensional-manifold of the phase space the matrix element has a zero. Then with increasing statistics, events closer and closer to this zero are generated, and feature larger and larger weights. Even though the contribution of such events to the weighted distribution is formally finite and integrable, the error estimate of the Monte Carlo generated distribution will not get reduced with the increasing statistical sample.

The tests were performed on a set of kinematic distributions: the pseudorapidity of outgoing parton j , rapidity of $\tau\tau$ and jj systems, invariant mass of $\tau\tau$ system, pseudorapidity of $\tau\tau$ system, opening angle between jets, opening angle between τ 's, angle between incoming parton and outgoing parton in the rest frame of jets and angle between resonance and outgoing parton in the rest frame of jets.

Plots for all these variables can be found on the web page [17]. Here, in Figs. 3 and 4, we present only plots for the difference of the jet's rapidities $\Delta\eta^{jj}$, the invariant mass of

the jet pair m^{jj} , the transverse momentum of τ pair $p_T^{\tau\tau}$ and, finally, the invariant mass of the τ -pair and jet-pair combined $m^{\tau\tau jj}$. In each plot the distribution Ref, for the reference process, is shown as a black histogram while the red histogram is the original distribution of generated events which are re-weighted using the TauSpinner $w_{\text{prod}}^{A\rightarrow B}$ weight to obtain the distribution represented by the red points with error bars. For the test to be successful, the red points should follow the black histogram; the ratio of Ref and re-weighted distributions is shown in the bottom panel of each figure.

In Figs. 3 and 4, the re-weighted distributions follow the Ref histograms. When re-weighting of X to H (see Fig. 4), the distributions feature larger statistical errors than in the case of H to X re-weighting (Fig. 3). This is simply because tight selection cuts leave only 1.7% of X events due to eliminating configurations with small m_{jj} . For some bins the re-weighted distribution lies below the target (black) distribution, whereas the ones with big errors tend to lie above it. If a similar feature appears when the sample size is increased it points to the possibility that the original distribution had a zero along some hyperspace. Nevertheless, if in distributions normalised to the cross section the neighbouring bins have no deficit of content, then the re-weighting algorithm can still be used.

The tests validating the re-weighting algorithm are completed with the ones monitoring the overall normalisations (integrated cross sections). For our samples and initialisations, the resulting cross sections are shown in Table 2. Reasonable agreement between cross sections obtained from the MadGraph5 calculation and with re-weighting was obtained; see Table 2 where the first line in the $H \rightarrow \tau\tau$ block should be compared with the second line in the $X \rightarrow \tau\tau$ block and vice versa. Such a study has to be repeated for each new matrix element implemented and whenever selection cuts are changed sizeably.

4.3 On reliability of the TauSpinner re-weighting approach

The TauSpinner re-weighting method is atypical compared to methods used in other tools, like REPOLO [29] PHYTIA [30], SHERPA. [31] or MadGraph [32]. Let us explain what the advantages and disadvantages are behind such a choice.

The advantage of our method is that it does not assume any knowledge of the initial and outgoing partons and tau leptons beyond their four-momenta. Therefore it can be applied directly to the experimental data, e.g. of the embedded τ samples. We have demonstrated that our re-weighting method is reliable for the hard process matrix elements convoluted with PDFs. The disadvantage is that it does not address the issue that both the parton shower and the hadronisation do depend on colour configuration as well as on flavours of partons. Once an event is re-weighted, the reshuffle between cate-

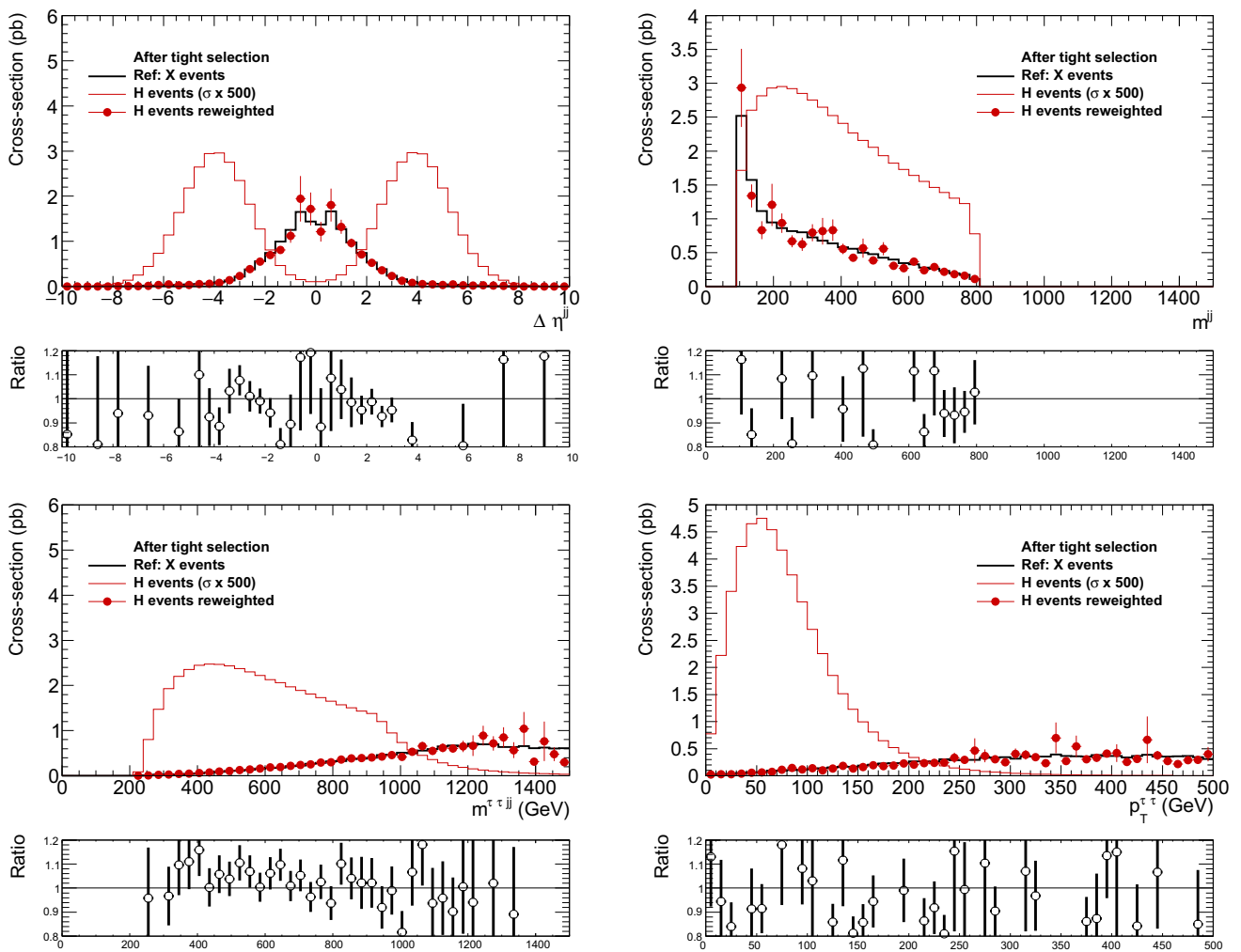


Fig. 3 The H sample re-weighted to the X and compared with the X sample. The H and X widths are 5.75 MeV. Selection cuts: Invariant mass of outgoing particles $m^{\tau\tau jj} < 1500$ GeV,

invariant mass of jets system $100 < m^{jj} < 800$ GeV and $p_T^{\tau\tau} < 600$ GeV. Variables on the x -axes as explained in Sect. 4.2

Table 2 Cross sections for the generated H production process and after its re-weighting to the X production ($H \rightarrow \tau\tau$ block), and for the generated X production and after its re-weighting to H production ($X \rightarrow \tau\tau$ block); acceptances with no, loose or tight selections applied for generated and re-weighted event samples are also shown

Events	No selection	Loose selection	Tight selection
$H \rightarrow \tau\tau$			
Acceptance	100%	73.8%	49.0%
σ [pb] (H)	$[2.033 \pm 0.064] 10^{-1}$	$[1.501 \pm 0.062] 10^{-1}$	$[1.004 \pm 0.045] 10^{-1}$
σ [pb] ($H \rightarrow X$)	$[9.097 \pm 1.270] 10^{+2}$	$[1.187 \pm 0.038] 10^{+2}$	$[1.517 \pm 0.066] 10^{+1}$
$X \rightarrow \tau\tau$			
Acceptance	100%	13.0%	1.71%
σ [pb] (X)	$[9.097 \pm 0.0029] 10^{+2}$	$[1.178 \pm 0.001] 10^{+2}$	$[1.544 \pm 0.004] 10^{+1}$
σ [pb] ($X \rightarrow H$)	$[2.023 \pm 0.0474] 10^{-1}$	$[1.478 \pm 0.031] 10^{-1}$	$[9.75 \pm 0.309] 10^{-2}$

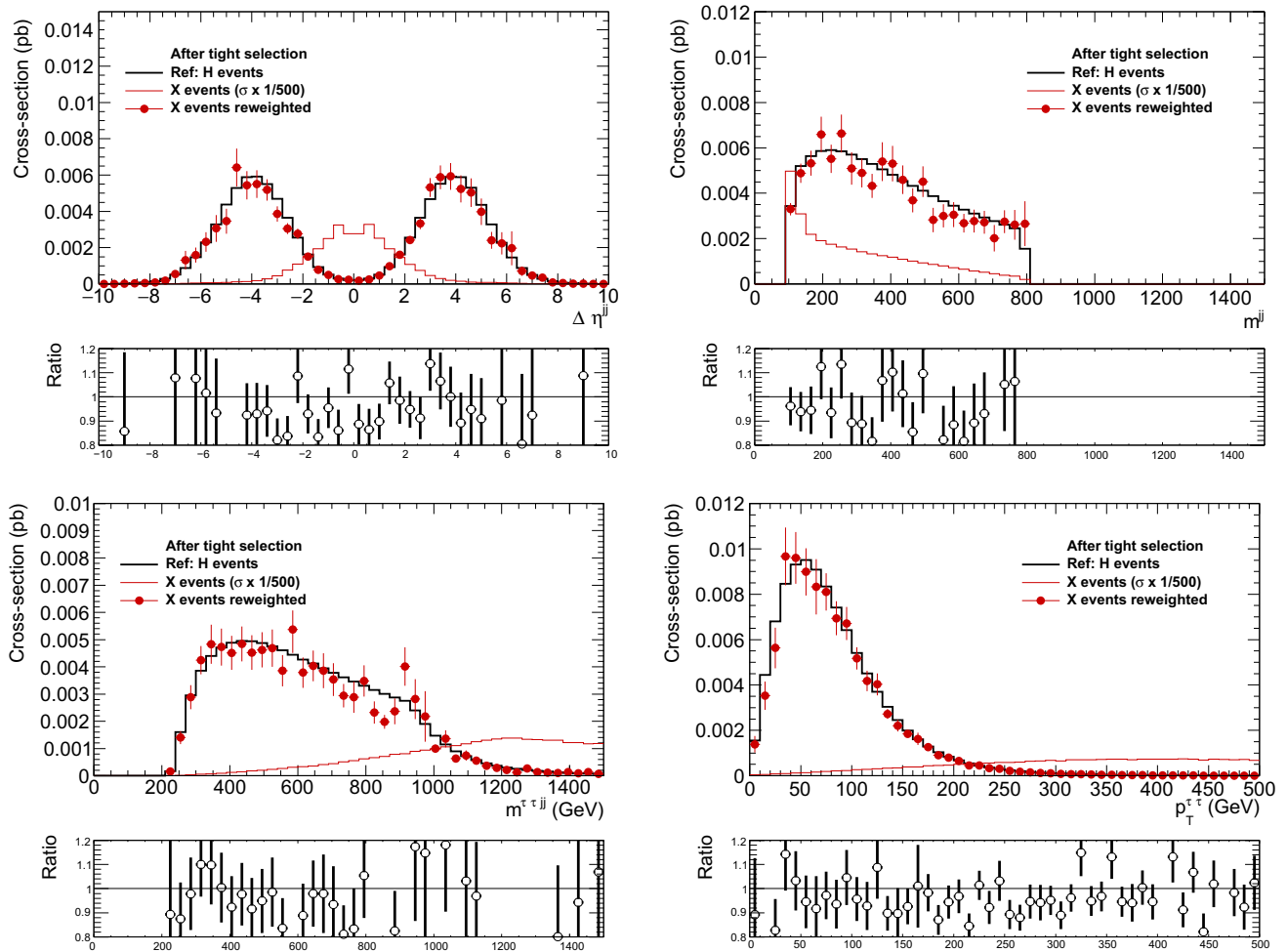


Fig. 4 The X sample re-weighted to the H and compared with the H sample. The H and X widths are 5.75 MeV. Selection cuts: invariant mass of outgoing particles $m^{\tau\tau jj} < 1500$ GeV, invariant mass of jets system $100 < m^{jj} < 800$ GeV and $p_T^{\tau\tau} < 600$ GeV. Note that statistical errors for the distributions obtained with re-weighting (red points) are

much larger than for the case of Fig. 3. This is predominantly due to small acceptance of the X sample: 1.7% only. But the agreement with the reference distribution (black histogram) remains within statistical fluctuation (dominated by large weight events). Variables on the x-axes as explained in Sect. 4.2

gories of different colour and/or flavour contents takes place, inevitably leading to biases.

In experimental simulation production files [33] colour information for the so-called truth entries is not stored. Even in the data formats prepared and agreed on by the community [34], such information, at best, consists of a connected tree, navigation inside of which retains information on the event history including the parents of unstable particles. There is an important caveat here: the event generators are modeling quantum processes, and the event record has the structure of a classical decay chain. It is inevitable that compromises must be made and difficulties can arise from an over-literal interpretation of the tree structure. For the colour it means that at best the so-called flow approximation is pre-imposed. Even for such partial information, there are no detailed commonly accepted rules for how it should be stored; see for example

Sect. 2.3 in [35] or Sect. 4.4.1 in the HepMC manual [36] or [37].

In practice, in experiment production files of detector response simulated events, information on intermediate quantum states is generally not available. Usually only the 4-momenta of partons and their flavours are stored. We are not in a position to affect these experiment choices. A multitude of arguments have been raised for such choices, including the fact that distinct generators prepared by theorists, provide such information in a different manner, or that it makes data files unnecessary large. We can only address the question if any useful solution for re-weighting may be designed⁵ and what kind of restrictions it implies have to be kept in mind.

⁵ Note that for spin effects we include in our re-weighting not only production matrix element, but the ones of τ 's decays as well.

There are two simulation steps which depend on hard process configurations of flavours and colours: parton shower and later hadronisation. It is well known that even mainstream Monte Carlo programs do not match in this respect sufficiently well the experimental data for all required phase-space regions [38]. This is a complex issue which we cannot exhaust.⁶

The discussion of the resulting systematic errors of our method is out of scope of the present paper. It would require the evaluation of how mismatches of the colour and flavour input for parton shower and hadronisation translates into reconstructed jets from simulated detector responses. This in turn would require the use of experimental detector response codes, not available publicly. In general, the `TauSpinner` application domain is restricted to observables where details of the jets, resulting from parton flavours or colour are not of importance. This has to be kept in mind.

Let us point out that our study examples of the previous sections are for the cases where starting and target distributions are massively different. In practical applications we expect `TauSpinner` to be used in configurations where new contributions to matrix elements are at the edge of observability.

If required, it is possible to apply `TauSpinner` in the flavour savvy manner. Possible solution may follow the method described in Appendix A. Contributions from distinct flavour configurations can be treated separately only for cases when in experiment production files the flavour configurations are stored or can be unwinded.

5 Spin dependent characteristics

So far we were discussing observables relying on the kinematics of final states consisting of four-momenta of τ leptons and accompanying two jets. Inclusion of τ decay products increase the phase-space dimensionality substantially, making the analysis much more difficult, especially when dependence on selection cuts is taken into account (as observed in the previous sections).

In the following, we will present a few spin dependent results obtained for the H and X samples within the tight selection cuts. Using `TAUOLA++` [41] we supplement these samples with τ decays in the simplest possible mode $\tau^\pm \rightarrow \pi^\pm \nu$ with no spin effects included. Spin effects are introduced with the help of `TauSpinner` weights, which are calculated according to the production and decay kinematics (see Refs. [1,42] for the spin weight definition).

⁶ A large effort is made to address this aspect of phenomenology thanks to new data analysis techniques. For example, new interesting results are obtained thanks to the machine learning approach [39,40].

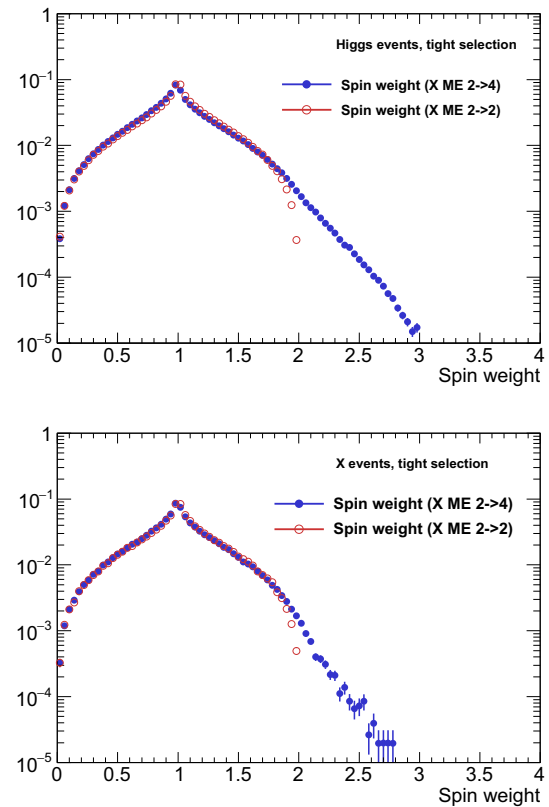


Fig. 5 Spin weight histograms, normalised to unity, obtained from X matrix elements for H sample (top plot) and X sample (bottom plot). In both cases samples are constrained with tight selection cuts. Red open circles are for when the effective Born ($2 \rightarrow 2$) matrix elements are used and blue full circle points are for when our new ($2 \rightarrow 4$) matrix elements are used

Figure 5 shows the spin weight histograms for the H and X samples. In both cases the spin weights are calculated first using the matrix element for X productions as described in Ref. [3], which is featuring effective Born $2 \rightarrow 2$ kinematics (open red circles), and they are compared with the new calculation in which amplitudes featuring two jet kinematics are taken into account (blue full circle points).⁷ In both cases the same $X - \tau\tau$ couplings were used. As expected (see Eq. (8) from Ref. [1]), for the $2 \rightarrow 2$ case the range of spin weights is limited to $[0, 2]$, since in this process there are no couplings which could lead to individual τ polarisation. In the $2 \rightarrow 4$ case the spin weight distribution exhibits a tail which extends beyond 2 and covers most of the allowed $[0, 4]$ range. This is due to, e.g., the presence of the subprocess $W^+W^- \rightarrow X \rightarrow \tau^+\tau^-$ in which W s radiated off quarks are polarised, which has impact on τ polarisation. The tail above 2, although not so much pronounced, will manifest itself in the distribution of τ decay products.

⁷ Here we exploit the virtue of `TauSpinner` which allows one, for a given sample, to calculate weights for different production mechanisms. This feature is of help in validating or rejecting theoretical hypotheses.

Let us now turn to the standard spin sensitive distribution of the ratio E_π/E_τ (a fraction of τ energy carried by the decay pion) used in [42] for benchmarking τ polarisation. In every case discussed below we will use again X production amplitudes to calculate τ pair density matrix. We will do that also for the sample generated with H production amplitudes.⁸

The τ polarisation can originate from the X production via VBF process, which is asymmetric over the phase-space regions due to the asymmetry of valence u and d quark distributions in the proton. To exhibit the polarisation effects we have to sort out events according to the τ polarisation; otherwise the effects will average out. Since in the proton there are more u -type quarks than d -type, the X particle produced in the VBF preferentially will follow the direction of the W^+ , which are right-handed and impart their polarisation on the X bosons. One can then expect that a τ lepton from X decay will have polarisation dependent on τ direction with respect to the X flight direction correlated with its spin polarisation. Thus it is suggestive of sorting events according to positive and negative values of $C = Y_X \cdot (p_z^{\tau^-} - p_z^{\tau^+})$, where Y_X denotes the τ lepton pair rapidity and $p_z^{\tau^-}, p_z^{\tau^+}$ are the z components of τ^\pm four-momenta. In Fig. 6 events with positive and negative C are plotted separately (the first bin for $C > 0$ is lower exhibiting the pion mass m_π/m_τ effect). We observe that spin weights, calculated with the X production amplitude, when applied to the H sample, lead to a larger spin effect than when applied to the X sample. In the second case the spin effect is barely visible.⁹

Our results illustrate the complexity of multi-dimensional distributions. Even within a tight selection there is a sizeable difference between events of X and H production, which is reflected in τ polarisation effects being greater for the H sample than for X sample, even though the same $pp \rightarrow \tau\tau jj$ matrix elements featuring intermediate X are used in both cases.

One could argue that such a small spin effect present in Fig. 6 for the X case is a consequence of a substantial contribution from other than VBF channel in our samples, thus hinting that our cuts may need to be refined. However, because of the weight distribution, as seen in the lower plot of Fig. 5, such a refinement is unlikely to be found within our tight selection, since the tail of events with spin weight exceeding 2 is very small. It seems that a better discriminating power between the $H \rightarrow \tau\tau$ and $X \rightarrow \tau\tau$ hypotheses can be provided by a longitudinal τ - τ spin correlation; the same as discussed already in Refs. [3,42]. Nonetheless τ polarisation may offer

⁸ Note that the separate treatment of τ production from the distributions of τ decay products enables evaluation of how important spin effects can be in experimental analyses.

⁹ It can be used nevertheless to improve the exclusion of a spin-2 hypothesis.

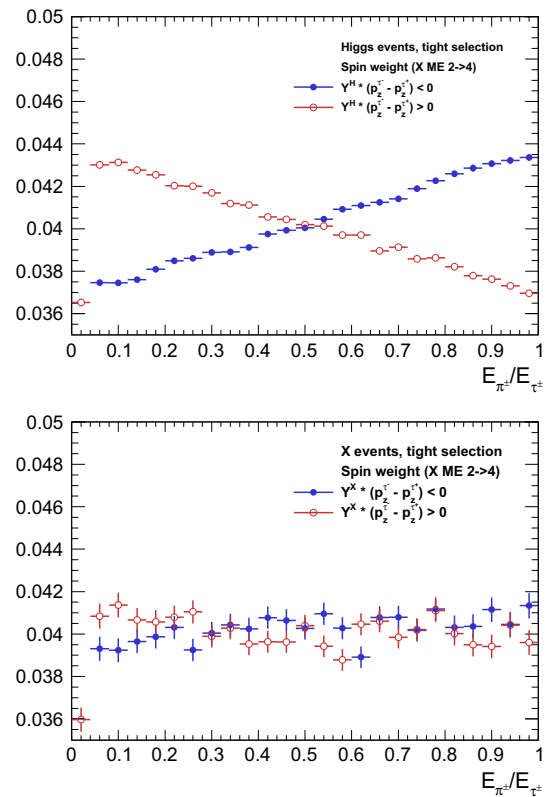


Fig. 6 Histograms of E_π/E_τ spectra, normalised to unity, for the H sample (top figure) and for the X sample (bottom figure). In all cases $2 \rightarrow 4$ matrix elements of X exchange are used to implement spin effects. Red open circle points are for additional cuts $Y_X \cdot (p_z^{\tau^-} - p_z^{\tau^+}) > 0$ and the blue, full circle points for $Y_X \cdot (p_z^{\tau^-} - p_z^{\tau^+}) < 0$. Note that because far less X events survive tight selection, statistical errors on the bottom plot are larger

(minor) help in the exclusion of the X hypothesis, even in the case when $X\tau\tau$ couplings are insensitive to parity.

6 Summary and outlook

The main purpose of the paper was to demonstrate how the new matrix elements for the production of τ -lepton pair accompanied by two jets in pp collisions (that is, new with respect to the ones used for sample generation) can be used in TauSpinner environment to re-weight events. For that purpose, the New Physics matrix element for a spin-2 X particle was implemented as a user example.

We have provided numerical tests of the algorithm, demonstrating that starting from the H sample (or the X sample), the other one can be obtained by applying event-by-event weight calculated from the implemented matrix elements. We have also addressed possible technical difficulties and limitations in implementing the user code for matrix elements. Even though the TauSpinner algorithm

in the case of its native and external matrix elements works similarly, technical aspects due to e.g. rounding errors and other numerical complications may differ; thus they require individual attention. The density of events to be re-weighted may differ from the target one significantly, resulting in a few events with weights massively larger than the ones from other regions of the phase space.

Limitations of the algorithm, discussed in Sect. 4.3, may be observed if for example colour or spin configurations for original and new process play an important role for the parton shower. Then re-weighting with the matrix element of a hard process only, see Eq. (2), may be too simplistic and factorisation properties may need to be addressed. An effort made in that direction can be found in Refs. [43,44].

Let us stress that the `TauSpinner` re-weighting can be repeated several times on the same event to obtain multiple variants of weights, e.g. due to several variants of coupling constants, or even completely distinct X interaction forms. In our examples we have used rather small sets of non-zero couplings, see Appendix B, in part to simplify the differences in the distributions of X and H mediated processes. The re-weighting algorithm performed better when a reduced region of the phase space was used for comparisons.

To demonstrate effects sensitive to the τ lepton polarisation we have chosen $\tau^\pm \rightarrow \pi^\pm \nu$ decay mode as a spin analyser. Spin effects originate from the X production vertex and are embedded in the complexity of the multi-body phase space. They turn out to be rather small for our choice of the $X\tau\tau$ couplings. Nevertheless, they may turn out to be useful in falsifying physics hypotheses alternative to Higgs production and decay processes.

This paper completes the description of `TauSpinner` functionality, initiated in [3] for the $2 \rightarrow 2$ matrix elements of New Physics, now also with the vector-boson-fusion $2 \rightarrow 4$ matrix elements. It supplements examples of `TauSpinner` applications for events with two jets accompanying τ -lepton pair production in pp collisions, discussed in [7].

Acknowledgements We thank Tomasz Przedziński for fruitful discussions and help with programming aspects of the `TauSpinner` code development. The work has been supported in part from funds of Polish National Science Center under decisions UMO-2014/15/B/ST2/00049, by PLGrid Infrastructure of the Academic Computer Centre CYFRONET AGH in Krakow, Poland (where the majority of the numerical calculations were performed) and by HARMONIA project under contract UMO-2015/18/M/ST2/00518 (2016–2019). MB, JK, ERW and ZW were supported in part by the Research Executive Agency (REA) of the European Union under the Grant Agreement PITNGA2012316704 (HiggsTools). WK was supported in part by the German DFG Grant STO 876/4-1. JK thanks the CERN Theoretical Physics Department for hospitality during the final stage of this work.

Open Access This article is distributed under the terms of the Creative Commons Attribution 4.0 International License (<http://creativecommons.org/licenses/by/4.0/>), which permits unrestricted use, distribution, and reproduction in any medium, provided you give appropriate credit

to the original author(s) and the source, provide a link to the Creative Commons license, and indicate if changes were made. Funded by SCOAP³.

Appendix A: Example with X mediated processes: user installation prototype

The purpose of this appendix is to present how the re-weighting with matrix elements of X mediated process, as available in the program distribution tar-ball, can be used. It is equally important to demonstrate how any other external matrix elements prepared by the user can be installed: the X case can serve as a prototype. The detailed instructions how the re-weighting algorithm works and how it can be used for final states of τ lepton pair and additional two jets is given already in Appendix A2 of Ref. [7]. In that paper, the non-Standard Model matrix elements were not discussed.

In the case of our example of spin-2 X mediated matrix elements, the command `TauSpinner::set_vbfdistr Modif(SPIN2::spin2distr);` is used to set the pointer to `SPIN2::spin2distr(...,KEY)`. This can be done for the user owned matrix-element routines. These routines should over-load the prototype ones for the non-standard calculation.

At initialisation, when the command `spin2init_()` is executed the masses and coupling constants for `SPIN2::spin2distr(...,KEY)` calculation are set. Later, for every event the algorithm makes the choice for the actual matrix elements used in the weight calculation: it evaluates and passes to the user-provided function its internal parameter `KEY`. The values `KEY = 0, 2` correspond to Drell–Yan-like processes of the Standard Model and an anomalous (user-provided) matrix element. Analogously `KEY = 1, 3` is for the Higgs of the Standard Model and (user-provided) matrix element for an anomalous narrow resonance. The code will choose between the Higgs and Drell–Yan background amplitudes on the basis of PDG identifier of the intermediate resonance found in the event record.¹⁰ For `X.pdgID ≠ 25` it will set `KEY=0` for Standard Model (A) – that is, for the denominator of $w_{\text{prod}}^{A \rightarrow B}$ given in Eq. (2) and `KEY=2` for (B), weight numerator. For `X.pdgID = 25` it will set `KEY=1` for (A) and `KEY=3` for (B). This is why a user-provided function for the matrix-element calculation must have a `KEY` parameter among its arguments.

The interface assumes that the event sample is for the SM; i.e. as of type (A) used in weight denominator while the user-provided function is of type (B), and accordingly the weight $w_{\text{prod}}^{A \rightarrow B}$ is calculated. If the analyzed event sample is (as for

¹⁰ Let us stress that `TauSpinner` assumes that the events sample used as an input is of the Standard Model type. It determines for every event whether it is of the Higgs type, by checking if the intermediate state `PDGid=25`. Otherwise, default Drell–Yan production will be assumed.

Fig. 4) of type (B), then the inverse of the weight given by Eq. (2) and calculated by TauSpinner should be used for re-weighting.

So far, we have not discussed spin polarisation and spin correlations between outgoing τ leptons. If a generated sample features spin correlations and polarisations of the τ leptons, then it has to be taken into account. The event weight needs to be supplemented with spin weights of the Standard Model and New Physics calculation,

$$w_{\text{prod}}^{A \rightarrow B} \rightarrow w_{\text{prod}}^{A \rightarrow B} \cdot \text{WT}/\text{WT0}, \quad (4)$$

where WT and WT0 denote the usual spin weight, as of Eq. (5) from Ref. [1], calculated first for (B) and then for (A). They can be obtained as shown in the extract from the code of the demonstration program.

A.1 Example of the demonstration program for X mediated processes

The detailed instruction for the demonstration program is given in Appendix A4 of Ref. [7]. However, some changes were required to allow the use of X mediated amplitudes and corresponding re-weighting. The distribution tar.ball [45] starting from the version of Jul. 11 2017, includes necessary provisions, which are commented out. For X mediated processes they have to be activated in the following files of the directory TAUOLA/TauSpinner/examples/example-VBF:

- the user example program `example-VBF.cxx`,
- the prototype `method_read_particles_for_VBF.cxx` to read in events stored in HepMC format, prepared specifically for MadGraph5 generated events,
- the SPIN2 directory which contains matrix elements,
- the README file in the TAUOLA/TauSpinner/examples/example-VBF/SPIN2, which contains all information for using the X matrix-elements implementation, which is as follows:
 - open Makefile in the SPIN2 directory and follow the instructions there,

- introduce a link to the SPIN2 library into configuration of TAUOLA/TauSpinner/examples

To activate the SPIN2 case in `example-VBF.cxx`:

- modify TAUOLA/TauSpinner/examples/Makefile: uncomment lines containing string SPIN2,
- modify TAUOLA/TauSpinner/examples/example-VBF/example-VBF.cxx: again look for commented lines which contain string spin2 or SPIN2 and uncomment them (note that `example-VBF.cxx` will use `methodTauSpinner::set_vbfdistrModif (SPIN2::spin2distr)`, but call on the `F77 spin2init_()` routine for initialisation of SPIN2 library constants is necessary),
- path to SPIN2 library has to be exported: `export LD_LIBRARY_PATH="/home...TAUOLA/TauSpinner/examples/example-VBF/SPIN2/lib:$LD_LIBRARY_PATH"`
- Makefile of SPIN2 directory has to be executed,
- the examples of TAUOLA/TauSpinner/examples and TAUOLA/TauSpinner/examples/example-VBF with SPIN2 library activated are ready to be compiled and linked.

For the user own external matrix elements, the scheme as of SPIN2 should be treated as a prototype which needs to be followed. The changes into the demonstration program `example-VBF.cxx` explained above provide necessary instructions. For further technical details we provide below an extract from the code.

A.2 Extract from the code `example-VBF.cxx`.

An extract from the TAUOLA/TauSpinner/examples/example-VBF/example-VBF.cxx file of the distribution tar-ball. Less important, at the first reading parts, are dropped. On the other hand, the code for a calculation of the spin weight contribution (Eq. (4)) is listed.

```

//-----
// For SPIN2 code placed in directory example-VBF:
// #include "spin2distr.h" // will work once 'export SPIN2LIB=...'
//-----
/** Example function that can be used to modify/replace matrix element calculation of vbfdist present in SPIN2/ME/
    spin2distr.cxx */
// double spin2distr(int I1, int I2, int I3, int I4, int H1, int H2, double P[6][4], int KEY, double vbfdistr_result)

int main(int argc, char **argv) {

    if(argc<2) {
        cout<<"Usage:  ``<<argv[0]<<'' <input_file> [<events_limit>]" << endl;
        cout<<"Consider: ``<<argv[0]<<'' events-VBF.dat 10" << endl;
        exit(-1);
    }

    char *input_filename = argv[1];
    int  events_limit  = 0;
    if(argc>2) events_limit = atoi(argv[2]);

    //-----
    //- Initialization -----
    //-----

    // Initialize Tauola
    Tauola::initialize();
    Tauola::spin_correlation.setAll(false);

    // Initialize random numbers:
    // ##1##
    // Important when you re-decay taus: set seed for tauola-fortran random number generator RANMAR
    // int ijklin=..., int ntotin=..., int ntot2n=...; /
    // Tauola::setSeed(ijklin,ntotin,ntot2n);
    // Tauola::setSeed(time(NULL), 0, 0);

    // ##2##
    // Important when you use attributed by TauSpinner helicities
    // Replace C++ Tauola Random generator with your own (take care of seeds). Prepared method:
    // gen.SetSeed(time(NULL));
    // Tauola::setRandomGenerator( randomik );

    // Initialize LHAPDF
    // string name="MSTW2008nnlo90cl.LHgrid";
    string name="cteq6ll.LHpdf";
    // choice used for events-VBF.lhe bring tiny variation, thus it is not
    // string name="MSTW2008nlo68cl.LHgrid"; // statistically important
    LHAPDF::initPDFSetByName(name);

    // CMSENE is the center of mass energy used in PDF calculations; only if Ipp = true
    // and only for Z/gamma*
    // Ipp - true for pp collision; otherwise polarization
    // of individual taus from Z/gamma* is set to 0.0

    // Ipol - relevant for Z/gamma* decays
    // 0 - events generated without spin effects
    // 1 - events generated with all spin effects
    // 2 - events generated with spin correlations and <pol>=0
    // 3 - events generated with spin correlations and
    // polarization but missing angular dependence of <pol>

    // nonSM2 option- 1/0 extra term in cross section, density matrix on/off
    // nonSMN option- 1/0 extra term in cross section, for shapes only on/off

    // For definition of EW and QCD schemes see Ref. [7].

    double CMSENE = 13000.0; // 14000.0;
    bool  Ipp      = true;
    int   Ipol     = 1;
    int   nonSM2   = 0;
    int   nonSMN   = 0;

    // Initialize TauSpinner
    initialize_spinner(Ipp, Ipol, nonSM2, nonSMN, CMSENE);

    int ref=1; // EW scheme to be used for default vbf calculation.
    int variant =1; // EW scheme to be used in optional matrix element reweighting (nonSM2=1). Then
    // for vbf calculation, declared above prototype method vbfdistrModif
    // (or user used).
    // At its disposal result of calculation with variant of EW scheme will be available.

```



```

vbfinit_(&ref,&variant);

int QCDdefault=1; // QCD scheme to be used for default vbf calculation.
int QCDvariant=1; // QCD scheme to be used in optional matrix element reweighting (nonSM2=1).
setPDFOpt(QCDdefault,QCDvariant);

// Set function that modifies/replaces Matrix Element calculation of vbf distr
// TauSpinner::set_vbfDistrModif(vbfDistrModif);

// Set function that modifies/replaces Matrix Element calculation of vbf distr with code of SPIN2
// spin2init_(&ref,&variant);
// TauSpinner::set_vbfDistrModif(SPIN2::spin2distr);

// Set function that modifies/replaces alpha_s calculation of vbf distr
// TauSpinner::set_alphasModif(alphasModif);

// Open I/O files (in our example events are taken from `events.dat`)
HepMC::IO_GenEvent input_file(input_filename,std::ios::in);

if(input_file.rdstate() ) {
    cout<<endl<<`ERROR: file `<<input_filename<<` not found.`<<endl<<endl;
    exit(-1);
}
int events_read =0;

int    events_count = 0;
double wt_sum      = 0.0;

//-----
// - Event loop -----
//-----
while( !input_file.rdstate() ) {
    double WT      = 1.0;
    double W[2][2] = { { 0.0 } };

    SimpleParticle p1, p2, X, p3, p4, tau1, tau2;
    vector<SimpleParticle> tau1_daughters, tau2_daughters;

    int status = read_particles_for_VBF(input_file,p1,p2,X,p3,p4,tau1,tau2,tau1_daughters,tau2_daughters);
    ++events_read;

    // WARNING: meaning of status may depend on the variant of read_particles_for_VBF().
    if( status == 1 ) break;           // variant A
    //      if ( status == 0 ) break;   // variant B
    //      else if( status == 1 ) { continue;} // variant B

    // setNonSMkey(0); // to calculate spin weight of Standard Model
    // double WT0 = calculateWeightFromParticlesVBF(p3, p4, X, tau1, tau2, tau1_daughters, tau2_daughters);

    // setNonSMkey(1); // e.g. for use of SPIN2 ME and calculate all weights
    WT = calculateWeightFromParticlesVBF(p3, p4, X, tau1, tau2, tau1_daughters, tau2_daughters);

    // double WTME=getWtNonSM(); // matrix element weight
    // WTME=WTME*WT/WT0; // factor to take into account spin correlations of tau-tau pair decays
    wt_sum += WT;
    ++events_count;
    if( events_count%100 == 0 ) cout << `EVT: ` << events_count << endl;
    if( events_limit && events_count >= events_limit ) break;
}

cout<<endl<<`No of events read from the file: `<<events_read<<endl;
cout<<endl<<`No of events processed for spin weight: `<<events_count<<endl;
cout<<      `WT average for these processed events: `<<wt_sum/events_count<<endl;

```

Appendix B: Details of MadGraph5 initialisation

The settings and parameters for the MadGraph5 [16] generation of H and spin-2 X event samples used in Sect. 4 are collected in the web page [17]. We remind the reader that these two generation parameter sets must be carefully matched with the corresponding ones in the initialisation of native TauSpinner (file `../TauSpinner/src/VBF/VBF_init.f`) and external matrix elements. In our example, it is the file `../TauSpinner/examples/example-VBF/SPIN2/ME/SPIN2_init.f`. A similar input consistency check will have to be performed whenever user-owned New Physics matrix elements are installed.

Let us recall some details how the code for matrix elements of X mediated processes were prepared. After the default (automatic) initialisation with MadGraph5 settings

```
set group_sub-processes Auto
set ignore_six_quark_processes False
set loop_optimized_output True
set low_mem_multicore_nlo_generation False
set loop_color_flows False
set gauge unitary
set complex_mass_scheme False
set max_npoint_for_channel 0
import model sm
define p = g u c d s u~ c~ d~ s~
define j = g u c d s u~ c~ d~ s~
define l+ = e+ mu+
define l- = e- mu-
define vl = ve vm vt
define vl~ = ve~ vm~ vt~
```

we produced the event generation code with the sets of commands given in Table 3.

The corresponding spin-2 `param_card.dat` file contains an additional block called `spin2` for model specific couplings.¹¹

```
Block spin2
  4 1.000000e+00 # gXtautauM
  5 1.000000e+00 # gXtautauP
  6 0.000000e+00 # gXqqM
  7 0.000000e+00 # gXqqP
  8 0.000000e+00 # gXggEven
  9 0.000000e+00 # gXggOdd
 10 1.000000e+00 # gXWWEven
 11 0.000000e+00 # gXWWOdd
 12 0.000000e+00 # gXBBEven
 13 0.000000e+00 # gXBBOdd
```

¹¹ Of the couplings of X to gauge bosons only the CP-even ones were implemented in the SPIN2 library. They are denoted in the code with a with suffix `Even` and correspond to couplings g_{Xii} , $i = B, W, g$, in Eq. (3).

as well as a block containing information as regards the quantum numbers [46] of the spin 2 object.

```
Block QNUMBERS 5000002 # x
  1 0 # 3 times electric charge
  2 5 # number of spin states (2S+1)
  3 1 # colour rep (1: singlet, 3:
      triplet, 8: octet)
  4 0 # Particle/Antiparticle
      distinction (0=own anti)
```

In addition, the block containing the Wolfenstein parametrisation of the CKM matrix is called `ckmblock` in the Spin-2 `param_card.dat` (as opposed to the name `wolfenstein` in the SM one).

The `run_card.dat` files used subsequently for generation of both H and X events are available from [17].

B.1 Setting precision parameter of MadGraph initialisation

The weights calculated with external new matrix elements may produce a tail of rare, high weight events. This may lead to excessively large statistical errors, sometimes poorly monitored in the histograms. Their origin is from sparsely populated phase-space regions in which some events receive high weight due to some resonance/collinear configuration of the new process; see, e.g., the discussion of Figs. 3 and 4 in Sect. 4.2 of Ref. [7].

Let us now comment on observations seemingly similar but of a fundamentally different origin.

In the early steps of tests, for re-weighting of X to H samples, we have encountered a mismatch between re-weighted and reference distributions generated in the gridpack mode. It turned out that the problem was related to the accuracy of samples generated by Madgraph5 based on MadEvent [47] algorithm. At the MadEvent core lies the diagram enhancement method which separates the integration into a sum of integrals whose singularity structure is dictated by a single Feynman diagram topology. Each of these individual integrals, referred to as integration channel, is then integrated using an appropriate phase-space parametrisation for its underlying structure. A MadEvent run involves two steps. The first one is referred to as the survey and consists of computing cross sections for each integration channel down to a given accuracy. Calling the `generate_events` script invokes a series of four commands: `survey`, `combine_events`, `store_events`, `create_gridpack`, in which by default `survey` should reach a precision of 0.01 within 8 iterations, where the first iteration consists of 2000 points. However, with this default iteration number the required accuracy of 0.01 was not achieved and the kinematical distributions for X samples did not show a good behavior. After invoking the four com-

Table 3 Commands to generate with the help of MadGraph5 the source code for H and X amplitudes calculation

Higgs	X
import model sm-ckm	import model spin2_w_CKM_UFO
generate p p > j j h QED=99, h > ta+ ta-	generate p p > j j x QCD=0 QED=2 NPVV=1 NPIL=1, x > ta+ ta-
output h_dir	output spin2_dir

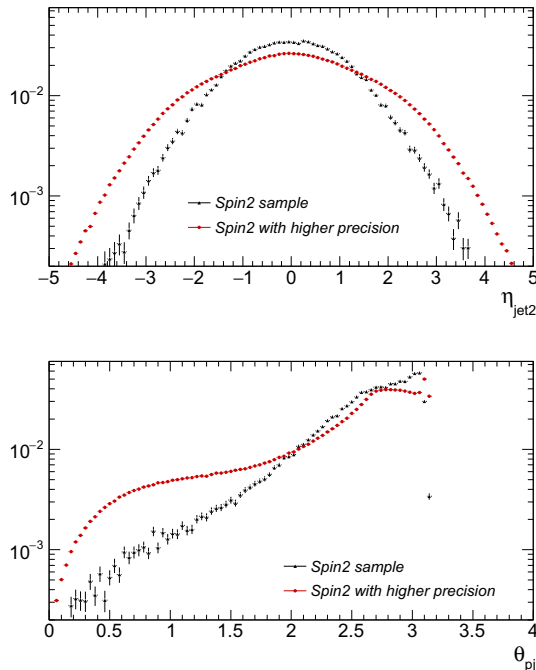


Fig. 7 Histograms of η_{jet2} and θ_{pj} distributions, normalised to unity, from MadGraph generated X samples. Black points are for the default 8 iterations used at initialisation, and red (grey) points for 99 iterations

mands one by one with the number of iterations in survey¹² increased to 99, the re-weighted distributions were matching the reference ones (as is the case of Figs. 3 and 4). One can see in Fig. 7 that the requirement for precision for the chosen distributions η_{jet2} and θ_{pj} turned out to be particularly demanding.

References

1. Z. Czczyula, T. Przedzinski, Z. Was, TauSpinner program for studies on spin effect in tau production at the LHC. *Eur. Phys. J.* **C72**, 1988 (2012). [arXiv:1201.0117](#)
2. ATLAS collaboration, G. Aad et al., Measurement of the WW cross section in $\sqrt{s} = 7$ TeV pp collisions with the ATLAS detector and limits on anomalous gauge couplings. *Phys. Lett.* **B712**, 289–308 (2012). [arXiv:1203.6232](#)

3. S. Banerjee, J. Kalinowski, W. Kotlarski, T. Przedzinski, Z. Was, Ascertaining the spin for new resonances decaying into tau+ tau- at Hadron Colliders. *Eur. Phys. J.* **C73**, 2313 (2013). [arXiv:1212.2873](#)
4. R. Józefowicz, E. Richter-Was, Z. Was, Potential for optimizing the Higgs boson CP measurement in $H \rightarrow \tau\tau$ decays at the LHC including machine learning techniques. *Phys. Rev.* **D94**, 093001 (2016). [arXiv:1608.02609](#)
5. E. Barberio, B. Le, E. Richter-Was, Z. Was, D. Zanzi, J. Zaremba, Deep learning approach to the Higgs boson CP measurement in H to tau tau decay and associated systematics. [arXiv:1706.07983](#)
6. Y. LeCun, Y. Bengio, G. Hinton, Deep learning. *Nature* **521**, 436–444 (2015)
7. J. Kalinowski, W. Kotlarski, E. Richter-Was and Z. Was, Production of τ lepton pairs with high p_T jets at the LHC and the TauSpinner reweighting algorithm. *Eur. Phys. J.* **C76**, 540 (2016). [arXiv:1604.00964](#)
8. M. Bahmani, J. Kalinowski, W. Kotlarski, E. Richter-Was, Z. Was, Systematic of TauSpinner for τ Pairs with two hard jets and its recent development. *Acta Phys. Pol. B* **48**, 903 (2017)
9. ATLAS collaboration, G. Aad et al., Search for neutral Higgs bosons of the minimal supersymmetric standard model in pp collisions at $\sqrt{s} = 8$ TeV with the ATLAS detector, *JHEP* **11**, 056 (2014). [arXiv:1409.6064](#)
10. CMS collaboration, Search for additional neutral Higgs bosons decaying to a pair of tau leptons in pp collisions at $\sqrt{s} = 7$ and 8 TeV, CMS-PAS-HIG-14-029
11. ATLAS collaboration, G. Aad et al., Measurement of τ polarization in $W \rightarrow \tau\nu$ decays with the ATLAS detector in pp collisions at $\sqrt{s} = 7$ TeV, *Eur. Phys. J.* **C72**, 2062 (2012). [arXiv:1204.6720](#)
12. CMS collaboration, Model independent search for Higgs boson pair production in the $b\bar{b}\tau^+\tau^-$ final state, CMS-PAS-HIG-15-013
13. V. Cherepanov, Measurement of the polarization of tau-leptons produced in Z decays at CMS and determination of the effective weak mixing angle. PhD thesis, Aachen, Tech. Hochsch. (2016)
14. ATLAS collaboration, G. Aad et al., Evidence for the Higgs-boson Yukawa coupling to tau leptons with the ATLAS detector, *JHEP* **04**, 117 (2015). [arXiv:1501.04943](#)
15. ATLAS collaboration, G. Aad et al., Modelling $Z \rightarrow \tau\tau$ processes in ATLAS with τ -embedded $Z \rightarrow \mu\mu$ data, *JINST* **10**, P09018 (2015). [arXiv:1506.05623](#)
16. J. Alwall, R. Frederix, S. Frixione, V. Hirschi, F. Maltoni, O. Mattelaer et al., The automated computation of tree-level and next-to-leading order differential cross sections, and their matching to parton shower simulations. *JHEP* **07**, 079 (2014). [arXiv:1405.0301](#)
17. M. Bahmani, J. Kalinowski, W. Kotlarski, E. Richter-Was, Z. Was. see <http://wasm.web.cern.ch/wasm/MadgraphIni.txt>. <http://wasm.web.cern.ch/wasm/MonitoringPlots.pdf>. <http://wasm.web.cern.ch/wasm/newprojects.html>
18. C.-W. Chiang, N.D. Christensen, G.-J. Ding, T. Han, Discovery in Drell–Yan processes at the LHC. *Phys. Rev.* **D85**, 015023 (2012). [arXiv:1107.5830](#)
19. P. Artoisenet et al., A framework for Higgs characterisation. *JHEP* **11**, 043 (2013). [arXiv:1306.6464](#)

¹² The syntax of setting survey options can be found by invoking the help_survey command in the madevent shell.

20. J. Frank, M. Rauch, D. Zeppenfeld, Spin-2 resonances in vector-boson-fusion processes at next-to-leading order QCD. *Phys. Rev. D* **87**, 055020 (2013). [arXiv:1211.3658](https://arxiv.org/abs/1211.3658)
21. ATLAS collaboration, G. Aad et al., Test of CP Invariance in vector-boson fusion production of the Higgs boson using the Optimal Observable method in the ditau decay channel with the ATLAS detector. *Eur. Phys. J.* **C76**, 658 (2016). [arXiv:1602.04516](https://arxiv.org/abs/1602.04516)
22. CMS collaboration, A.M. Sirunyan et al., Observation of the Higgs boson decay to a pair of tau leptons. [arXiv:1708.00373](https://arxiv.org/abs/1708.00373)
23. G. Das, C. Degrande, V. Hirschi, F. Maltoni, H.-S. Shao, NLO predictions for the production of a spin-two particle at the LHC. *Phys. Lett.* **B770**, 507–513 (2017). [arXiv:1605.09359](https://arxiv.org/abs/1605.09359)
24. A. Alloul, N.D. Christensen, C. Degrande, C. Duhr, B. Fuks, FeynRules 2.0—a complete toolbox for tree-level phenomenology. *Comput. Phys. Commun.* **185**, 2250–2300 (2014). [arXiv:1310.1921](https://arxiv.org/abs/1310.1921)
25. C. Degrande, C. Duhr, B. Fuks, D. Grellscheid, O. Mattelaer, T. Reiter, UFO—the universal FeynRules output. *Comput. Phys. Commun.* **183**, 1201–1214 (2012). [arXiv:1108.2040](https://arxiv.org/abs/1108.2040)
26. K. Hagiwara, J. Kanzaki, Q. Li, K. Mawatari, HELAS and MadGraph/MadEvent with spin-2 particles. *Eur. Phys. J. C* **56**, 435–447 (2008). [arXiv:0805.2554](https://arxiv.org/abs/0805.2554)
27. P. de Aquino, W. Link, F. Maltoni, O. Mattelaer, T. Stelzer. *Comput. Phys. Commun.* **183**, 2254 (2012). <https://doi.org/10.1016/j.cpc.2012.05.004>. [arXiv:1108.2041](https://arxiv.org/abs/1108.2041) [hep-ph]
28. I. Antcheva et al., *Comput. Phys. Commun.* **180**, 2499 (2009). <https://doi.org/10.1016/j.cpc.2009.08.005>. [arXiv:1508.07749](https://arxiv.org/abs/1508.07749) [physics.data-an]
29. F. Schissler. https://www.itp.kit.edu/vbfnlo/wiki/lib/exe/fetch.php?media=documentation:repolo_1.0.pdf
30. S. Mrenna, P. Skands, *Phys. Rev. D* **94**(7), 074005 (2016). <https://doi.org/10.1103/PhysRevD.94.074005>. [arXiv:1605.08352](https://arxiv.org/abs/1605.08352) [hep-ph]
31. E. Bothmann, M. Scoenherr, S. Schumann, *Eur. Phys. J. C* **76**(11), 590 (2016). <https://doi.org/10.1140/epjc/s10052-016-4430-0>. [arXiv:1606.08753](https://arxiv.org/abs/1606.08753) [hep-ph]
32. P. Artoisenet, V. Lemaître, F. Maltoni, O. Mattelaer, *JHEP* **1012**, 068 (2010). [https://doi.org/10.1007/JHEP12\(2010\)068](https://doi.org/10.1007/JHEP12(2010)068). [arXiv:1007.3300](https://arxiv.org/abs/1007.3300) [hep-ph]
33. G. Aad et al. [ATLAS Collaboration], *Eur. Phys. J. C* **70**, 823 (2010). <https://doi.org/10.1140/epjc/s10052-010-1429-9>. [arXiv:1005.4568](https://arxiv.org/abs/1005.4568) [physics.ins-det]
34. see e.g. <http://hepmc.web.cern.ch/hepmc/>. Accessed 3 Jan 2018
35. M. Dobbs, J.B. Hansen, *Comput. Phys. Commun.* **134**, 41 (2001). [https://doi.org/10.1016/S0010-4655\(00\)00189-2](https://doi.org/10.1016/S0010-4655(00)00189-2)
36. The manual can be found in http://hepmc.web.cern.ch/hepmc/releases/HepMC2_user_manual.pdf. Accessed 3 Jan 2018
37. J. Alwall et al., *Comput. Phys. Commun.* **176**, 300 (2007). <https://doi.org/10.1016/j.cpc.2006.11.010>. [arXiv:hep-ph/0609017](https://arxiv.org/abs/hep-ph/0609017)
38. G. Aad et al. [ATLAS Collaboration], *Eur. Phys. J. C* **76**(6), 322 (2016). <https://doi.org/10.1140/epjc/s10052-016-4126-5>. [arXiv:1602.00988](https://arxiv.org/abs/1602.00988) [hep-ex]
39. A.J. Larkoski, I. Moulton, B. Nachman. [arXiv:1709.04464](https://arxiv.org/abs/1709.04464) [hep-ph]
40. E.M. Metodiev, B. Nachman, J. Thaler, *JHEP* **1710**, 174 (2017). [https://doi.org/10.1007/JHEP10\(2017\)174](https://doi.org/10.1007/JHEP10(2017)174). [arXiv:1708.02949](https://arxiv.org/abs/1708.02949) [hep-ph]
41. N. Davidson, G. Nanava, T. Przedzinski, E. Richter-Was, Z. Was, *Comput. Phys. Commun.* **183**, 821 (2012). <https://doi.org/10.1016/j.cpc.2011.12.009>. [arXiv:1002.0543](https://arxiv.org/abs/1002.0543) [hep-ph]
42. A. Kaczmarska, J. Piatlicki, T. Przedzinski, E. Richter-Was, Z. Was, *Acta Phys. Polon.* **B45**(10), 1921 (2014). <https://doi.org/10.5506/APhysPolB.45.1921>. [arXiv:1402.2068](https://arxiv.org/abs/1402.2068) [hep-ph]
43. E. Richter-Was, Z. Was, Separating electroweak and strong interactions in Drell–Yan processes at LHC: leptons angular distributions and reference frames. *Eur. Phys. J. C* **76**, 473 (2016). [arXiv:1605.05450](https://arxiv.org/abs/1605.05450)
44. E. Richter-Was, Z. Was, W production at LHC: lepton angular distributions and reference frames for probing hard QCD. *Eur. Phys. J. C* **77**, 111 (2017). [arXiv:1609.02536](https://arxiv.org/abs/1609.02536)
45. N. Davidson et al., 2008–2017, the up-to-date tar-ball for the source code and documentation of Tauola and TauSpinner see <http://wasm.web.cern.ch/wasm/c++.html> or <http://tauolapp.web.cern.ch>
46. J. Alwall et al., A Les Houches interface for BSM generators. <https://doi.org/10.2172/921331>. [arXiv:0712.3311](https://arxiv.org/abs/0712.3311) [hep-ph]
47. F. Maltoni, T. Stelzer, MadEvent: automatic event generation with MadGraph. *JHEP* **0302**, 027 (2003). [arXiv:hep-ph/0208156](https://arxiv.org/abs/hep-ph/0208156)